

Efficient Parallel-in-Time Solution of Time-Periodic Problems Using a Multi-Harmonic Coarse Grid Correction

Iryna Kulchytska-Ruchka^{a,*}, Sebastian Schöps^a

^a*Institut für Teilchenbeschleunigung und Elektromagnetische Felder, Technische Universität Darmstadt, Schlossgartenstrasse 8, D-64289 Darmstadt, Germany*

Abstract

This paper presents a highly-parallelizable parallel-in-time algorithm for efficient solution of (non-linear) time-periodic problems. It is based on the time-periodic extension of the Parareal method, known to accelerate sequential computations via parallelization on the fine grid. The proposed approach reduces complexity of the periodic Parareal solution by introducing a special simplified Newton algorithm, which allows an additional parallelization on the coarse grid. In particular, at each Newton iteration a multi-harmonic correction is performed, which converts the block-cyclic periodic system in the time domain into a block-diagonal system in the frequency domain, thereby allowing separate solution for each frequency component in parallel. Comparison of the introduced algorithm and several existing solution approaches is illustrated via their application to the eddy current problem for both linear and nonlinear models of a coaxial cable.

Keywords: Time-periodic problems, parallelization in time, Parareal algorithm, frequency domain solution, fast Fourier transform

1. Introduction

The computation of the time-periodic solution of an evolution problem becomes particularly relevant, when one is interested in the steady-state behavior of a dynamical system such as, e.g., an electrical machine. Numerical treatment of time-periodic problems is often challenging since it requires a simultaneous solution of the underlying system on the whole period. Indeed, a classical methodology involves a finite element method (FEM) discretization in space followed by a finite

*Corresponding author

Email addresses: kulchytska@temf.tu-darmstadt.de (Iryna Kulchytska-Ruchka), schoeps@temf.tu-darmstadt.de (Sebastian Schöps)

difference discretization in time, which couples all the discrete values on one period through the periodicity condition. This space-time discretization approach of time-periodic problems is known in engineering as the time-periodic finite element method (TP-FEM) [1]. It leads to a large system of algebraic equations whose solution would usually be very computationally expensive or even prohibitive, especially due to its troublesome block-cyclic structure. These obstacles on the way to solve time-periodic problems cause an urgent need to develop efficient algorithms, able to simplify and accelerate the time-domain computations.

Based on the idea of the multiple shooting method [2], the Parareal algorithm was originally introduced to speed up sequential solution of initial value problems (IVPs) using parallelization in the time domain [3]. It involves computations on two grids: the fine and the coarse. While the coarse solver gives a rough information about the solution and is applied sequentially, the acceleration is obtained via parallel calculation of the accurate fine solution. Convergence properties of the method were investigated in [4], [5]. Application of Parareal to the simulation of an electrical machine in [6] illustrated its significant acceleration capabilities. The original Parareal approach for IVPs was subsequently extended to the class of time-periodic problems and analyzed in [7].

Here we consider a Parareal-based iterative algorithm to solve time-periodic problems using parallelization on both fine and coarse levels [8]. The method exploits the frequency domain solution approach from [9], which we call the multi-harmonic (MH) solver throughout this paper, exploiting the terminology used in [10]. It is applied to the coarse time-periodic Parareal system, thereby allowing to calculate each frequency component separately and in parallel. Application of the fast Fourier transform [11] makes this parallel-in-time approach particularly attractive due to its low complexity. This work extends the ideas in [9], [8] by introducing a simplified Newton iteration, which allows to solve also problems with nonlinearities efficiently using the described MH technique. The convergence of the method is analyzed and discussed specifically for the case of the eddy current problem.

Our paper is organized as follows. At first, a couple of existing parallel-in-time approaches for time-periodic problems [7] are described in Section 2. Section 3 recalls the main ideas of the frequency domain solution [9] as well as its parallel-in-time extension presented in [8]. A special iterative method is then introduced in Section 4 for solution of nonlinear time-periodic problems with the MH approach. Application of the proposed method to numerical treatment of the eddy current problem, as well as its performance compared to the conventional sequential time stepping,

to the time-parallel algorithms from [7], and to the MH solution of [9] are presented in Section 5. The paper is finally concluded with Section 6.

2. Periodic Parareal-based parallel-in-time algorithms

Consider a time-periodic problem for a system of ordinary differential equations (ODEs) on time interval $(0, T)$

$$\begin{aligned} \mathbf{M}\mathbf{u}'(t) + \mathbf{K}(\mathbf{u}(t))\mathbf{u}(t) &= \mathbf{j}(t), \quad t \in (0, T), \\ \mathbf{u}(0) &= \mathbf{u}(T), \end{aligned} \tag{1}$$

with positive definite matrices \mathbf{M} and $\mathbf{K}(\mathbf{u}(t))$, where \mathbf{K} depends on unknown $\mathbf{u} : [0, T] \rightarrow \mathbb{R}^d$ and $\mathbf{j} : [0, T] \rightarrow \mathbb{R}^d$ is a T -periodic right-hand side (RHS). System (1) could stem, e.g., from a spatial discretization of a parabolic partial differential equation (PDE) with FEM [12].

As in the classical Parareal method [3], we initially split the time interval $[0, T]$ into N subintervals $[T_{n-1}, T_n]$, $n = 1, \dots, N$ using partition $0 = T_0 < T_1 < \dots < T_N = T$. An IVP for unknown $\mathbf{u}_n : [T_{n-1}, T_n] \rightarrow \mathbb{R}^d$ such that

$$\begin{aligned} \mathbf{M}\mathbf{u}'_n(t) + \mathbf{K}(\mathbf{u}_n(t))\mathbf{u}_n(t) &= \mathbf{j}(t), \quad t \in (T_{n-1}, T_n], \\ \mathbf{u}_n(T_{n-1}) &= \mathbf{U}_{n-1} \end{aligned} \tag{2}$$

is then considered on n th subinterval, $n = 1, \dots, N$. Within the Parareal setting, two propagators are applied to the n th IVP: the fine $\mathcal{F}(\cdot, T_{n-1}, \mathbf{U}_{n-1})$ and the coarse $\mathcal{G}(\cdot, T_{n-1}, \mathbf{U}_{n-1})$, [4]. Both operators calculate a solution to (2) on $(T_{n-1}, T_n]$, starting from initial value \mathbf{U}_{n-1} at T_{n-1} , $n = 1, \dots, N$. However, the accuracies and therefore the computational costs of the two solvers differ. In particular, \mathcal{F} solves the IVP with a very high precision, e.g., via time stepping over a very fine grid, while \mathcal{G} provides only a rough approximation of the solution, e.g., by using a very coarse discretization or a lower-order method, compared to the fine propagator.

Based on the idea of Parareal, [7] introduces two parallel-in-time algorithms for efficient treatment of time-periodic problems. The first one, called periodic Parareal algorithm with initial-value coarse problem (PP-IC), calculates the periodic solution using iteration

$$\mathbf{U}_0^{(k+1)} = \mathbf{U}_N^{(k)}, \tag{3}$$

$$\mathbf{U}_n^{(k+1)} = \mathcal{F}(T_n, T_{n-1}, \mathbf{U}_{n-1}^{(k)}) + \mathcal{G}(T_n, T_{n-1}, \mathbf{U}_{n-1}^{(k+1)}) - \mathcal{G}(T_n, T_{n-1}, \mathbf{U}_{n-1}^{(k)}) \tag{4}$$

for $k = 0, 1, \dots$ and $n = 1, \dots, N$. While in the classical Parareal method the initial value (at T_0) is fixed, (3)-(4) updates the solution at T_0 with the solution at T_N , obtained from the previous iteration. In this way PP-IC weakens the direct periodic coupling among the discrete values at the synchronization points T_n , $n = 0, \dots, N - 1$ and, like Parareal, involves solution of IVPs on the coarse level. The method has been recently applied to simulation of an induction motor for an electric vehicle drive by the authors in [13] and already delivered a significant speedup. However, since PP-IC imposes a relaxed periodicity constraint one could possibly expect a rather slow convergence to the periodic solution, especially when the underlying dynamical system possesses a very long settling time.

The second approach presented in [7] is PP-PC: periodic Parareal algorithm with periodic coarse problem. In contrast to PP-IC, it maintains the prescribed periodic coupling between the first and the last values of the period $[T_0, T_N]$. The PP-PC iterations are written for $k = 0, 1, \dots$ as follows:

$$\mathbf{U}_0^{(k+1)} = \mathcal{F}(T_N, T_{N-1}, \mathbf{U}_{N-1}^{(k)}) + \mathcal{G}(T_N, T_{N-1}, \mathbf{U}_{N-1}^{(k+1)}) - \mathcal{G}(T_N, T_{N-1}, \mathbf{U}_{N-1}^{(k)}), \quad (5)$$

$$\mathbf{U}_n^{(k+1)} = \mathcal{F}(T_n, T_{n-1}, \mathbf{U}_{n-1}^{(k)}) + \mathcal{G}(T_n, T_{n-1}, \mathbf{U}_{n-1}^{(k+1)}) - \mathcal{G}(T_n, T_{n-1}, \mathbf{U}_{n-1}^{(k)}) \quad (6)$$

with $n = 1, \dots, N - 1$. It can be seen that the fine solutions only involve values from iteration k and can therefore be computed in parallel, in the same way as within Parareal and PP-IC. On the other hand, the coarse propagation cannot as before be performed sequentially, since the periodicity condition yields interconnection of the solution at the synchronization points. Hence, PP-PC requires solution of a periodic coarse problem, which requires a joint computation of the coarse grid values over the whole period.

Denoting the difference between the fine and the coarse solutions of IVP (2) at T_n , calculated starting from initial value $\mathbf{U}_{n-1}^{(k)}$ at T_{n-1} , by

$$\mathbf{b}_n^{(k)} = \mathcal{F}(T_n, T_{n-1}, \mathbf{U}_{n-1}^{(k)}) - \mathcal{G}(T_n, T_{n-1}, \mathbf{U}_{n-1}^{(k)}), \quad n = 1, \dots, N \quad (7)$$

we write PP-PC iteration (5)-(6) in a matrix-vector (operator) form

$$\begin{bmatrix} \mathbf{I} & \mathbf{0} & \dots & -\mathcal{G}(T_N, T_{N-1}, \cdot) \\ -\mathcal{G}(T_1, T_0, \cdot) & \mathbf{I} & & \mathbf{0} \\ \vdots & \ddots & \ddots & \vdots \\ \mathbf{0} & \dots & -\mathcal{G}(T_{N-1}, T_{N-2}, \cdot) & \mathbf{I} \end{bmatrix} \begin{bmatrix} \mathbf{U}_0^{(k+1)} \\ \mathbf{U}_1^{(k+1)} \\ \vdots \\ \mathbf{U}_{N-1}^{(k+1)} \end{bmatrix} = \begin{bmatrix} \mathbf{b}_N^{(k)} \\ \mathbf{b}_1^{(k)} \\ \vdots \\ \mathbf{b}_{N-1}^{(k)} \end{bmatrix}, \quad (8)$$

where $\mathbf{I} \in \mathbb{R}^{d \times d}$ denotes the identity matrix. Note that the system matrix of (8) might have large dimensions, since each of the unknown $\mathbf{U}_n^{(k+1)}$, $n = 0, \dots, N-1$ possibly consists of many degrees of freedom coming from the spatial discretization. The matrix also possesses a block-cyclic structure, which is typical for time-periodic systems but inconvenient for many linear solvers.

System (8) is written in an implicit operator form and cannot be solved directly in the nonlinear case. A Jacobi-type fixed point iteration was applied in [7] to iteratively solve the PP-PC system. It is written for $s = 0, 1, \dots$ as

$$\begin{bmatrix} \mathbf{U}_0^{(k+1,s+1)} \\ \mathbf{U}_1^{(k+1,s+1)} \\ \vdots \\ \mathbf{U}_{N-1}^{(k+1,s+1)} \end{bmatrix} = \begin{bmatrix} \mathbf{0} & \mathbf{0} & \dots & \mathcal{G}(T_N, T_{N-1}, \cdot) \\ \mathcal{G}(T_1, T_0, \cdot) & \mathbf{0} & & \mathbf{0} \\ \vdots & \ddots & \ddots & \vdots \\ \mathbf{0} & \dots & \mathcal{G}(T_{N-1}, T_{N-2}, \cdot) & \mathbf{0} \end{bmatrix} \begin{bmatrix} \mathbf{U}_0^{(k+1,s)} \\ \mathbf{U}_1^{(k+1,s)} \\ \vdots \\ \mathbf{U}_{N-1}^{(k+1,s)} \end{bmatrix} + \begin{bmatrix} \mathbf{b}_N^{(k)} \\ \mathbf{b}_1^{(k)} \\ \vdots \\ \mathbf{b}_{N-1}^{(k)} \end{bmatrix} \quad (9)$$

at each PP-PC iteration $k+1$. The fixed point iteration (9) decouples calculation of the values $\mathbf{U}_n^{(k+1,s+1)}$, $n = 0, \dots, N-1$ completely, thereby allowing parallel solution even on the coarse level. On the other hand, it relaxes the periodicity constraint similarly to PP-IC and might therefore be not efficient in some cases. Besides, for a linear problem (9) does not converge in a single iteration, as one would naturally expect from a linearization approach, but the parallelizability comes with an additional inner loop in s . Our aim is to construct an iterative method, which would benefit from the present block-cyclic structure and provide a faster convergence.

3. Frequency domain solution for time-periodic (Parareal) systems

Frequency domain representation is often exploited in (electrical) engineering due to its property of transforming a differential equation into an algebraic one [14]. In contrast to the possibly lengthy time stepping in the time domain, MH frequency domain computations allow to obtain the steady-state solution directly via calculating its harmonic components. However, it may require many basis functions if the solution exhibits local features, e.g., due to pulsed excitations [18]. This frequency domain solution approach is also called the harmonic balance method [15], [16] and can be interpreted as the Fourier collocation [17] or the Fourier spectral method [11].

3.1. Multi-harmonic approach

The main idea of the MH solution [9] lies in representation of a periodic function $u \in L^2([0, T], \mathbb{C})$ from Lebesgue space $L^2([0, T], \mathbb{C})$ (for the definition we refer to [19, Chapter 23.2]) by the infinite sum

$$u(t) = \sum_{j=-\infty}^{\infty} \hat{u}_j \psi_j(t), \quad t \in [0, T]$$

of the spectral (orthonormal) basis functions $\psi_j(t) = e^{i2\pi jt/T}$ on time interval $[0, T]$, with (Fourier) coefficients

$$\hat{u}_j := \frac{1}{T} \int_0^T u(t) \psi_j^*(t) dt = \frac{1}{T} \int_0^T u(t) e^{-i2\pi jt/T} dt, \quad j \in \mathbb{Z}. \quad (10)$$

Searching for T -periodic solution u (i.e., $u(0) = u(T)$) of an ODE

$$F(u', u, t) = 0, \quad t \in (0, T), \quad (11)$$

we write its variational formulation

$$0 = (F(u', u, t), \psi)_{L^2([0, T], \mathbb{C})} := \frac{1}{T} \int_0^T F(u', u, t) \psi^*(t) dt \quad \forall \psi \in L^2([0, T], \mathbb{C}) \quad (12)$$

where it is assumed that $u' \in L^2([0, T], \mathbb{C}^*)$, with \mathbb{C}^* denoting the dual space of the space of complex numbers \mathbb{C} . The unknown solution u is then approximated with the finite Fourier series

$$u(t) \approx \sum_{j=1}^N \hat{u}_j e^{i\omega_j t}, \quad t \in [0, T] \quad (13)$$

using frequencies

$$\omega_j = 2\pi p_j/T, \quad j = 1, \dots, N \quad (14)$$

from the double-sided spectrum given by N -dimensional vector

$$\vec{p} = [-\lfloor N/2 \rfloor + \delta, \dots, \lfloor N/2 \rfloor]^T \in \mathbb{R}^N, \quad (15)$$

where

$$\delta = \begin{cases} 1, & \text{if } N \text{ is even} \\ 0, & \text{if } N \text{ is odd} \end{cases}$$

and $\lfloor \cdot \rfloor$ denotes the floor function, which returns the greatest integer less than or equal to its argument. This yields a finite-dimensional system of equations

$$0 = \frac{1}{T} \int_0^T \hat{F}(\hat{\mathbf{u}}, t) e^{-i\omega_j t} dt, \quad j = 1, \dots, N \quad (16)$$

with respect to the unknown coefficients $\hat{\mathbf{u}} = [\hat{u}_1, \dots, \hat{u}_N]^\top$ in the frequency domain. Here $\hat{F}(\hat{\mathbf{u}}, t)$ denotes the restriction of $F(u', u, t)$ in (11) after substitution of u from (13) therein. Using the calculated frequency components \hat{u}_j , expansion (13) gives the solution in the time domain. Note that approximation of (10) using the left rectangle quadrature rule on a partition $0 = T_0 < T_1 < \dots < T_{N-1} < T$

$$\hat{u}_j = \frac{1}{N} \sum_{n=0}^{N-1} u(T_n) e^{-i\omega_j T_n}, \quad j = 1, \dots, N \quad (17)$$

is the discrete Fourier transform (DFT) of vector $\mathbf{u} = [u(T_0), \dots, u(T_{N-1})]^\top$, while (13) evaluated at $t = T_n$, $n = 0, 1, \dots, N-1$ gives the inverse DFT of $\hat{\mathbf{u}}$. In the following subsection we exploit the MH discretization idea to solve PP-PC system (8) for a linear time-periodic problem.

3.2. Multi-harmonic approach for linear PP-PC system

We now describe the MH approach [9] applied to parallel-in-time solution of a linear (non-autonomous) problem of the form

$$\begin{aligned} \mathbf{M}\mathbf{u}'(t) + \mathbf{K}\mathbf{u}(t) &= \mathbf{j}(t), \quad t \in (0, T), \\ \mathbf{u}(0) &= \mathbf{u}(T) \end{aligned} \quad (18)$$

with matrices \mathbf{M} and \mathbf{K} such that $(\mathbf{M} + \mathbf{K})$ is non-singular and RHS $\mathbf{j}(t)$. Discretization by the implicit Euler method on the equidistant coarse grid $0 = T_0 < T_1 < \dots < T_N = T$ defines the coarse solution $\mathcal{G}(T_n, T_{n-1}, \mathbf{U}_{n-1})$ at T_n by

$$\underbrace{\left[\frac{1}{\Delta T} \mathbf{M} + \mathbf{K} \right]}_{=: \mathbf{Q}} \mathcal{G}(T_n, T_{n-1}, \mathbf{U}_{n-1}) = \underbrace{\frac{1}{\Delta T} \mathbf{M}}_{=: \mathbf{C}} \mathbf{U}_{n-1} + \mathbf{j}(T_n), \quad n = 1, \dots, N \quad (19)$$

with step size $\Delta T = T/N$. This yields PP-PC system (8) in explicit matrix-vector form

$$\underbrace{\begin{bmatrix} \mathbf{Q} & & & -\mathbf{C} \\ -\mathbf{C} & \mathbf{Q} & & \\ & \ddots & \ddots & \\ & & -\mathbf{C} & \mathbf{Q} \end{bmatrix}}_{=:\mathbf{G}} \begin{bmatrix} \mathbf{U}_0^{(k+1)} \\ \mathbf{U}_1^{(k+1)} \\ \vdots \\ \mathbf{U}_{N-1}^{(k+1)} \end{bmatrix} = \underbrace{\begin{bmatrix} \mathbf{r}_N^{(k)} \\ \mathbf{r}_1^{(k)} \\ \vdots \\ \mathbf{r}_{N-1}^{(k)} \end{bmatrix}}_{=:\mathbf{r}^{(k)}}, \quad (20)$$

where the RHS is defined by

$$\mathbf{r}_n^{(k)} := \mathbf{Q}\mathbf{b}_n^{(k)} + \mathbf{j}(T_n)$$

and vector $\mathbf{b}_n^{(k)}$, $n = 1, \dots, N$ is given by (7). Originating from (8), system matrix \mathbf{G} has the same troublesome block-cyclic structure. The MH solution approach [9] overcomes this difficulty by decoupling the solution on the coarse level without introducing an additional iteration, in contrast to (9).

Since $\mathbf{U}_0^{(k+1)}, \dots, \mathbf{U}_{N-1}^{(k+1)}$ are values of a periodic function at T_0, \dots, T_{N-1} one could express them with the finite Fourier series expansion (13) discretized at the synchronization points, i.e.,

$$\mathbf{U}_n^{(k+1)} = \sum_{j=1}^N \hat{\mathbf{U}}_j^{(k+1)} e^{i\omega_j T_n}, \quad n = 0, \dots, N-1, \quad (21)$$

with frequencies ω_j given by (14). Plugging (21) into PP-PC system (20) and applying DFT (17) gives an equivalent system in frequency domain

$$\underbrace{\left(\tilde{\mathbf{F}} \mathbf{G} \tilde{\mathbf{F}}^H \right)}_{=:\hat{\mathbf{G}}} \hat{\mathbf{U}}^{(k+1)} = \underbrace{\tilde{\mathbf{F}} \mathbf{r}^{(k)}}_{=:\hat{\mathbf{r}}^{(k)}} \quad (22)$$

in terms of the unknown Fourier coefficients $\hat{\mathbf{U}}_j^{(k+1)}$, $j = 1, \dots, N$ contained in the joint vector $\hat{\mathbf{U}}^{(k+1)} \in \mathbb{C}^{Nd}$. Matrix $\tilde{\mathbf{F}}$ is defined by $\tilde{\mathbf{F}} = \mathbf{F} \otimes \mathbf{I}$, where \mathbf{F} is the DFT matrix with elements

$$\mathbf{F}_{jq} = e^{-i\omega_j T_{q-1}} / \sqrt{N}, \quad j, q = 1, \dots, N, \quad (23)$$

\mathbf{I} is a $d \times d$ -dimensional identity matrix, and ' \otimes ' denotes the Kronecker product of two matrices. $\tilde{\mathbf{F}}^H$ is the Hermite conjugate matrix of $\tilde{\mathbf{F}}$.

We emphasize that the transformation from (20) to (22) comes along with an important property: it transforms the block-cyclic system matrix \mathbf{G} into the block-diagonal system matrix $\hat{\mathbf{G}}$. Matrices on the diagonal of $\hat{\mathbf{G}}$ can be explicitly calculated as

$$\hat{\mathbf{G}}_{jj} = \mathbf{Q} - \mathbf{C}e^{-i\Delta T\omega_j}, \quad j = 1, \dots, N. \quad (24)$$

This allows to find each harmonic component independently by solving

$$\hat{\mathbf{G}}_{jj} \hat{\mathbf{U}}_j^{(k+1)} = \hat{\mathbf{r}}_j^{(k)}, \quad j = 1, \dots, N. \quad (25)$$

One therefore has a possibility of an additional parallelization on the coarse level, i.e., solution of N systems of d linear equations could be performed in parallel, without introduction of an additional inner loop. Note that matrices $\tilde{\mathbf{F}}$ and $\tilde{\mathbf{F}}^H$ do not have to be explicitly constructed, since the system matrices in (25) for each frequency ω_j are determined by (24).

Solution in the time domain can be obtained by application of the inverse DFT to the calculated solution vector $\hat{\mathbf{U}}^{(k+1)}$, i.e.,

$$\mathbf{U}^{(k+1)} = \tilde{\mathbf{F}}^H \hat{\mathbf{U}}^{(k+1)}. \quad (26)$$

Note that the DFT and its inverse can be calculated efficiently using the fast Fourier transform algorithm [11], thereby further reducing the complexity of the transformation.

4. Periodic parareal-in-time algorithm with multi-harmonic coarse grid correction

We now consider the following time-periodic problem for a system of nonlinear differential equations

$$\begin{aligned} \mathbf{M}\mathbf{u}'(t) + \mathbf{K}(\mathbf{u}(t))\mathbf{u}(t) &= \mathbf{j}(t), \quad t \in (0, T), \\ \mathbf{u}(0) &= \mathbf{u}(T) \end{aligned} \quad (27)$$

with nonlinearity present in matrix $\mathbf{K}(\mathbf{u}(t))$, e.g., due to nonlinear material characteristics. Similarly to (20), coarse discretization with implicit Euler's method on an equidistant grid leads to the PP-PC system

$$\begin{bmatrix} \mathbf{Q}_N(\mathbf{U}_{N-1}^{(k+1)}) & & & -\mathbf{C} \\ -\mathbf{C} & \mathbf{Q}_1(\mathbf{U}_0^{(k+1)}) & & \\ & \ddots & \ddots & \\ & & -\mathbf{C} & \mathbf{Q}_{N-1}(\mathbf{U}_{N-2}^{(k+1)}) \end{bmatrix} \begin{bmatrix} \mathbf{U}_0^{(k+1)} \\ \mathbf{U}_1^{(k+1)} \\ \vdots \\ \mathbf{U}_{N-1}^{(k+1)} \end{bmatrix} = \begin{bmatrix} \mathbf{r}_N(\mathbf{U}_{N-1}^{(k+1)}) \\ \mathbf{r}_1(\mathbf{U}_0^{(k+1)}) \\ \vdots \\ \mathbf{r}_{N-1}(\mathbf{U}_{N-2}^{(k+1)}) \end{bmatrix} \quad (28)$$

with the following definitions

$$\begin{aligned} \mathbf{Q}_n(\mathbf{U}_{n-1}^{(k+1)}) &:= \mathbf{C} + \mathbf{K}(\mathcal{G}(T_n, T_{n-1}, \mathbf{U}_{n-1}^{(k+1)})), \quad \mathbf{C} := \frac{1}{\Delta T} \mathbf{M}, \\ \mathbf{r}_n(\mathbf{U}_{n-1}^{(k+1)}) &:= \mathbf{Q}_n(\mathbf{U}_{n-1}^{(k+1)}) \mathbf{b}_n^{(k)} + \mathbf{j}(T_n), \quad n = 1, \dots, N, \end{aligned}$$

where $\mathbf{b}_n^{(k)}$, $n = 1, \dots, N$ is given by (7) and $\Delta T = T/N$. Substituting $\mathcal{G}(T_n, T_{n-1}, \mathbf{U}_{n-1}^{(k+1)})$, $n = 1, \dots, N$ from PP-PC iteration (5)-(6) into (28) and omitting superscript $k+1$ we obtain the following nonlinear system for $\mathbf{U} = [\mathbf{U}_0^\top, \dots, \mathbf{U}_{N-1}^\top]^\top$

$$\underbrace{\begin{bmatrix} \mathbf{Q}(\mathbf{U}_0 - \mathbf{b}_N^{(k)}) & & & -\mathbf{C} \\ -\mathbf{C} & \mathbf{Q}(\mathbf{U}_1 - \mathbf{b}_1^{(k)}) & & \\ & \ddots & \ddots & \\ & & -\mathbf{C} & \mathbf{Q}(\mathbf{U}_{N-1} - \mathbf{b}_{N-1}^{(k)}) \end{bmatrix}}_{=:\mathbf{G}(\mathbf{U})} \begin{bmatrix} \mathbf{U}_0 \\ \mathbf{U}_1 \\ \vdots \\ \mathbf{U}_{N-1} \end{bmatrix} = \underbrace{\begin{bmatrix} \mathbf{r}_N(\mathbf{U}_0) \\ \mathbf{r}_1(\mathbf{U}_1) \\ \vdots \\ \mathbf{r}_{N-1}(\mathbf{U}_{N-1}) \end{bmatrix}}_{=:\mathbf{r}(\mathbf{U})} \quad (29)$$

where

$$\begin{aligned} \mathbf{Q}(\mathbf{X}) &:= \mathbf{C} + \mathbf{K}(\mathbf{X}), \quad \mathbf{X} \in \mathbb{R}^d, \quad \mathbf{C} := \frac{1}{\Delta T} \mathbf{M}, \\ \mathbf{r}_n(\mathbf{U}_m) &:= \mathbf{Q}(\mathbf{U}_m - \mathbf{b}_n^{(k)}) \mathbf{b}_n^{(k)} + \mathbf{j}(T_n), \quad 1 \leq n \leq N, \quad 0 \leq m \leq N-1, \end{aligned}$$

with $\mathbf{b}_n^{(k)}$, $n = 1, \dots, N$ from (7). To solve (29) we search for the root of mapping $\mathbf{R} : \mathbb{R}^{Nd} \rightarrow \mathbb{R}^{Nd}$ defined by

$$\mathbf{R}(\mathbf{U}) = \begin{bmatrix} \mathbf{Q}(\mathbf{U}_0 - \mathbf{b}_N^{(k)})[\mathbf{U}_0 - \mathbf{b}_N^{(k)}] - \mathbf{C}\mathbf{U}_{N-1} - \mathbf{j}(T_N) \\ \mathbf{Q}(\mathbf{U}_1 - \mathbf{b}_1^{(k)})[\mathbf{U}_1 - \mathbf{b}_1^{(k)}] - \mathbf{C}\mathbf{U}_0 - \mathbf{j}(T_1) \\ \vdots \\ \mathbf{Q}(\mathbf{U}_{N-1} - \mathbf{b}_{N-1}^{(k)})[\mathbf{U}_{N-1} - \mathbf{b}_{N-1}^{(k)}] - \mathbf{C}\mathbf{U}_{N-2} - \mathbf{j}(T_{N-1}) \end{bmatrix} \quad (30)$$

using the simplified Newton iteration [17]: for $s = 0, 1, \dots$ solve

$$\mathbf{J}_{\mathbf{R}}(\mathbf{U}^0) \mathbf{U}^{s+1} = -[\mathbf{R}(\mathbf{U}^s) - \mathbf{J}_{\mathbf{R}}(\mathbf{U}^0) \mathbf{U}^s]. \quad (31)$$

Jacobian matrix $\mathbf{J}_{\mathbf{R}}$ is defined by

$$\mathbf{J}_{\mathbf{R}}(\mathbf{U}) = \frac{d}{d\mathbf{U}} \mathbf{R}(\mathbf{U}) = \begin{bmatrix} \mathbf{Q}_d(\mathbf{U}_0 - \mathbf{b}_N^{(k)}) & & & -\mathbf{C} \\ -\mathbf{C} & \mathbf{Q}_d(\mathbf{U}_1 - \mathbf{b}_1^{(k)}) & & \\ & \ddots & \ddots & \\ & & -\mathbf{C} & \mathbf{Q}_d(\mathbf{U}_{N-1} - \mathbf{b}_{N-1}^{(k)}) \end{bmatrix} \quad (32)$$

where

$$\mathbf{Q}_d(\mathbf{X}) = \mathbf{C} + \mathbf{K}_d(\mathbf{X}), \quad \mathbf{K}_d(\mathbf{X}) = \frac{d}{d\mathbf{X}} [\mathbf{K}(\mathbf{X}) \mathbf{X}], \quad \mathbf{X} \in \mathbb{R}^d. \quad (33)$$

With the choice of initial approximation at PP-PC iteration $k + 1$

$$\mathbf{U}^0 := \left[(\mathbf{Z} + \mathbf{b}_N^{(k)})^\top, (\mathbf{Z} + \mathbf{b}_1^{(k)})^\top, \dots, (\mathbf{Z} + \mathbf{b}_{N-1}^{(k)})^\top \right]^\top \quad (34)$$

for a given vector $\mathbf{Z} \in \mathbb{R}^d$ simplified Newton's iteration (31) reads

$$\mathbf{G}_d \mathbf{U}^{s+1} = \mathbf{h}^s \quad (35)$$

with system matrix

$$\mathbf{G}_d = \begin{bmatrix} \mathbf{Q}_d(\mathbf{Z}) & & & & -\mathbf{C} \\ -\mathbf{C} & \mathbf{Q}_d(\mathbf{Z}) & & & \\ & & \ddots & & \\ & & & \ddots & \\ & & & & -\mathbf{C} & \mathbf{Q}_d(\mathbf{Z}) \end{bmatrix} \quad (36)$$

and RHS $\mathbf{h}^s := -[\mathbf{R}(\mathbf{U}^s) - \mathbf{G}_d \mathbf{U}^s]$. The matrix remains constant over the Newton iterations and has the same block-cyclic structure as that of PP-PC system (20) for the linear problem. Hence, a MH solver can be also applied to the Newton system (35). Analogously to (22) we obtain

$$\underbrace{(\tilde{\mathbf{F}} \mathbf{G}_d \tilde{\mathbf{F}}^H)}_{=:\hat{\mathbf{G}}_d} \hat{\mathbf{U}}^{s+1} = \tilde{\mathbf{F}} \mathbf{h}^s, \quad (37)$$

where matrix $\hat{\mathbf{G}}_d$ is block-diagonal with each $(d \times d)$ -dimensional block given by

$$[\hat{\mathbf{G}}_d]_{jj} = \mathbf{Q}_d(\mathbf{Z}) - \mathbf{C} e^{-i\Delta T \omega_j}, \quad j = 1, \dots, N \quad (38)$$

and the DFT matrix $\tilde{\mathbf{F}}$ is as previously defined by (23). The frequency domain solution $\hat{\mathbf{U}}^{s+1}$ at Newton iteration $s + 1$ is then transformed into the time domain by the inverse DFT, i.e.,

$$\mathbf{U}^{s+1} = \tilde{\mathbf{F}}^H \hat{\mathbf{U}}^{s+1}. \quad (39)$$

Remark 4.1. We note that the simplified Newton iteration (31) could be also interpreted as a linear iterative method based on an additive splitting of the system matrix in (29). Indeed, using any constant matrix $\mathbf{H} \in \mathbb{R}^{Nd \times Nd}$ we can introduce a linear iteration for $s = 0, 1, \dots$

$$\mathbf{H} \mathbf{U}^{s+1} = [\mathbf{H} - \mathbf{G}(\mathbf{U}^s)] \mathbf{U}^s + \mathbf{r}(\mathbf{U}^s). \quad (40)$$

Setting $\mathbf{H} = \mathbf{J}_R(\mathbf{U}^0)$ it can then be easily seen using (29) and (30) that the fixed point iteration (40) is exactly the iteration formula which generates iterates \mathbf{U}^{s+1} in (31).

4.1. Convergence analysis

Convergence of the simplified Newton method (31) is determined by the result presented in [17, Theorem 2.5], which originates from [20]. We recall the theorem here in terms of the notations introduced above.

Theorem 4.2 (Convergence of the simplified Newton method [17]). *Let $\mathbf{R} : D \rightarrow \mathbb{R}^d$ be a continuously differentiable mapping with $D \subset \mathbb{R}^d$ open and convex. Let $\mathbf{U}^0 \in D$ denote a given starting point so that $\mathbf{J}_{\mathbf{R}}(\mathbf{U}^0)$ is invertible. Assume the affine covariant Lipschitz condition*

$$\left\| \mathbf{J}_{\mathbf{R}}(\mathbf{U}^0)^{-1} [\mathbf{J}_{\mathbf{R}}(\mathbf{U}) - \mathbf{J}_{\mathbf{R}}(\mathbf{U}^0)] \right\| \leq \delta_0 \|\mathbf{U} - \mathbf{U}^0\| \quad (41)$$

holds for all $\mathbf{U} \in D$. Let

$$h_0 := \delta_0 \|\mathbf{U}^1 - \mathbf{U}^0\| \leq 0.5 \quad (42)$$

and assume that the closure $\bar{S}(\mathbf{U}^0, \rho)$ of a ball with center in \mathbf{U}^0 and radius $\rho = (1 - \sqrt{1 - 2h_0}) / \delta_0$ is a subset of D . Then the simplified Newton iterates \mathbf{U}^{s+1} , $s = 0, 1, \dots$ generated by (31) remain in $\bar{S}(\mathbf{U}^0, \rho)$ and converge to some \mathbf{U}^* with $\mathbf{R}(\mathbf{U}^*) = \mathbf{0}$.

Remark 4.3. *When the matrix \mathbf{H} in (40) is chosen such that it has the form of the original system matrix in the PP-PC system (29) and contains constant equal block-matrices on the diagonal, i.e.,*

$$\mathbf{H} = \mathbf{G}(\mathbf{U}_{\mathbf{Z}}) \quad \text{with} \quad \mathbf{U}_{\mathbf{Z}} := \left[\mathbf{Z}^\top, \mathbf{Z}^\top, \dots, \mathbf{Z}^\top \right]^\top \quad \text{for some} \quad \mathbf{Z} \in \mathbb{R}^d, \quad (43)$$

then even global convergence of the fixed point iteration (40) could be derived under special boundedness conditions imposed on the nonlinearity in (27).

Without loss of generality, we discuss the convergence analysis of the simplified Newton iteration (31) for the PP-PC algorithm applied to a time-periodic problem for a single ($d = 1$) ODE. For a specific physically motivated nonlinearity we consider

$$\begin{aligned} mu'(t) + \kappa(|u|)u(t) &= j(t), \quad t \in (0, T), \\ u(0) &= u(T), \end{aligned} \quad (44)$$

with $m \in \mathbb{R}_0^+$, $\kappa : \mathbb{R}_0^+ \rightarrow \mathbb{R}_0^+$, unknown function $u : [0, T] \rightarrow \mathbb{R}$, and T -periodic input j , i.e., $j(0) = j(T)$.

Analogously to (32) the Jacobian matrix for this one-dimensional (1D) problem is determined by

$$\mathbf{J}_{\mathbf{R}}(\mathbf{U}) = \begin{bmatrix} c + \kappa_d(u_0 - b_N^{(k)}) & & & & -c \\ & -c & c + \kappa_d(u_1 - b_1^{(k)}) & & \\ & & \ddots & \ddots & \\ & & & -c & c + \kappa_d(u_{N-1} - b_{N-1}^{(k)}) \end{bmatrix}, \quad (45)$$

where $\mathbf{U} = [u_0, \dots, u_{N-1}]^\top$, $c = m/\Delta T$ with $\Delta T = T/N$, and for $x \in \mathbb{R}$

$$\kappa_d(x) = [\kappa(|x|x)]' = \begin{cases} \kappa'(|x|)|x| + \kappa(|x|), & x \neq 0, \\ \kappa(0), & x = 0. \end{cases} \quad (46)$$

As in (34) choosing a fixed value $z \in \mathbb{R}$ we define

$$\mathbf{U}^0 := [z + b_N^{(k)}, z + b_1^{(k)}, \dots, z + b_{N-1}^{(k)}]^\top \quad (47)$$

to be the initial approximation for the Newton iteration at PP-PC iteration $k + 1$. We denote the Jacobian matrix $\mathbf{J}_{\mathbf{R}}$ at the chosen \mathbf{U}^0 from (47) by \mathbf{G}_d which is given by

$$\mathbf{G}_d = \begin{bmatrix} c + \kappa_d(z) & & & & -c \\ & -c & c + \kappa_d(z) & & \\ & & \ddots & \ddots & \\ & & & -c & c + \kappa_d(z) \end{bmatrix} \quad (48)$$

Due to its special structure \mathbf{G}_d can be decomposed as

$$\mathbf{G}_d = \mathbf{F}^H \hat{\mathbf{G}}_d \mathbf{F}, \quad (49)$$

with unitary DFT matrix \mathbf{F} defined in (23) and diagonal matrix $\hat{\mathbf{G}}_d$ containing eigenvalues of \mathbf{G}_d .

This implies

$$\|\mathbf{G}_d^{-1}\|_2 = \left\| \left(\mathbf{F}^H \hat{\mathbf{G}}_d \mathbf{F} \right)^{-1} \right\|_2 = \left\| \hat{\mathbf{G}}_d^{-1} \right\|_2 = \max_{1 \leq j \leq N} \left| \left[\kappa_d(z) + (1 - e^{-i\Delta T \omega_j}) c \right]^{-1} \right|, \quad (50)$$

where $\|\cdot\|_2 = \sigma_{\max}(\cdot)$ denotes the largest singular value of a matrix, which for a normal matrix such as \mathbf{G}_d^{-1} is equal to its spectral radius. Using (50) we have for the Lipschitz condition (41) that

$$\begin{aligned} \left\| \mathbf{J}_{\mathbf{R}}(\mathbf{U}^0)^{-1} [\mathbf{J}_{\mathbf{R}}(\mathbf{U}) - \mathbf{J}_{\mathbf{R}}(\mathbf{U}^0)] \right\|_2 &\leq \|\mathbf{G}_d^{-1}\|_2 \|\mathbf{J}_{\mathbf{R}}(\mathbf{U}) - \mathbf{J}_{\mathbf{R}}(\mathbf{U}^0)\|_2 = \\ &\max_{1 \leq j \leq N} \left| \left[\kappa_d(z) + (1 - e^{-i\Delta T \omega_j}) c \right]^{-1} \right| \max_{\substack{1 \leq n \leq N \\ 0 \leq m \leq N-1}} \left| \kappa_d(u_m - b_n^{(k)}) - \kappa_d(z) \right|. \end{aligned} \quad (51)$$

To show (local) convergence of the simplified Newton method (31) one has to prove that expression (51) can be estimated by $\delta_0 \|\mathbf{U} - \mathbf{U}^0\|_2$, $\delta_0 > 0$ from above.

Theorem 4.4. *If the function $\kappa_d : \mathbb{R} \mapsto \mathbb{R}_0^+$ given in (46) is*

- *bounded from below, i.e.,*

$$\exists c_1 > 0 : \quad \kappa_d(x) \geq c_1 \quad \forall x \in \mathbb{R}, \quad (52)$$

- *Lipschitz continuous, i.e.,*

$$\exists c_2 > 0 : \quad |\kappa_d(x) - \kappa_d(y)| \leq c_2|x - y| \quad \forall x, y \in \mathbb{R}, \quad (53)$$

then the affine covariant Lipschitz condition (41) holds for (51) with constant $\delta_0 = c_2/c_1$.

Proof. Indeed, due to (52) and since $c \in \mathbb{R}_0^+$ we have for $1 \leq j \leq N$

$$\begin{aligned} \left| \left[\kappa_d(z) + (1 - e^{-\imath \Delta T \omega_j})c \right]^{-1} \right| &\leq \left[\Re \left(\kappa_d(z) + (1 - e^{-\imath \Delta T \omega_j})c \right) \right]^{-1} \\ &= \left[\kappa_d(z) + (1 - \cos(\Delta T \omega_j))c \right]^{-1} \leq [\kappa_d(z)]^{-1} \leq \frac{1}{c_1}. \end{aligned} \quad (54)$$

Using (53) and (54) in expression (51) we directly obtain estimate (41) with $\delta_0 = c_2/c_1$. \square

Provided the initial approximation \mathbf{U}^0 from (47) is sufficiently close to the sought root of a nonlinear mapping of form (30) such that (42) holds, Theorem 4.4 then implies local convergence of the simplified Newton method (31), derived in terms of the conditions imposed on function κ_d . In the following two lemmas using the results of [21] we state which properties of the function κ itself are sufficient such that (52) and (53) hold for κ_d .

Lemma 4.5. *If for $\kappa : \mathbb{R}_0^+ \mapsto \mathbb{R}_0^+$ it holds that*

- $\kappa(t) \geq c_1$, $t \in \mathbb{R}_0^+$,
- *function $t \mapsto \kappa(t)t$ is strongly monotone with monotonicity constant c_1 , i.e.,*

$$(\kappa(t)t - \kappa(s)s)(t - s) \geq c_1(t - s)^2 \quad \forall t, s \in \mathbb{R}_0^+, \quad (55)$$

which implies that $[\kappa(t)t]' \geq c_1$, $t \in \mathbb{R}_0^+$,

then function κ_d defined in (46) has a lower bound c_1 , i.e., it satisfies (52).

Lemma 4.6. *Assuming for $\kappa : \mathbb{R}_0^+ \mapsto \mathbb{R}_0^+$ it holds that*

- $\kappa \in C^1(\mathbb{R}_0^+)$ and $\lim_{t \rightarrow \infty} \kappa'(t) = 0$, which implies that κ is Lipschitz continuous with Lipschitz constant $\kappa_2 := \sup_{t \in \mathbb{R}_0^+} |\kappa'(t)|$, i.e.,

$$|\kappa(t) - \kappa(s)| \leq \kappa_2 |t - s| \quad \forall t, s \in \mathbb{R}_0^+, \quad (56)$$

- function $t \mapsto \kappa'(t)t$ is Lipschitz continuous, i.e.,

$$\exists L_2 > 0 : |\kappa'(t)t - \kappa'(s)s| \leq L_2 |t - s| \quad \forall t, s \in \mathbb{R}_0^+, \quad (57)$$

we have that Lipschitz continuity (53) of κ_d is satisfied with Lipschitz constant $c_2 = \kappa_2 + L_2$.

Condition (41) is then satisfied based on the assumptions of Lemmas 4.5 and 4.6, in the same way as in Theorem 4.4, which implies convergence of the simplified Newton iteration (31) according to Theorem 4.2. However, one should be aware of the fact that it may not always be possible to find an initial guess \mathbf{U}^0 which is at the same time close enough to the solution for convergence of the Newton iteration and has the form (47) for applicability of the MH solver to system (35) with constant matrix \mathbf{G}_d . Nevertheless, in those cases a fixed point iteration of form (40) may still be used.

Remark 4.7. *We would like to note that restriction to the 1D case does not bound the generality of our convergence statement. In particular, extension to a d -dimensional problem (27), obtained from a spatial discretization of a PDE, could be based on the operator theory provided in [21]. In this case one would need to consider the properties not only of function κ but also of a nonlinear operator $A : V \mapsto V^*$, which, e.g., for a diffusion equation with nonlinear diffusion coefficient $\kappa(|\nabla u|)$ is defined as*

$$\langle A(u), v \rangle_{V^*, V} = (\kappa(|\nabla u|) \nabla u, \nabla v)_H \quad \forall u, v \in V, \quad (58)$$

with a reflexive Banach space V and Hilbert space H , e.g., $V = H_0^1(\Omega)$ and $H = L^2(\Omega)$ on domain Ω . We refer to [21, Corollary 2.13, Theorem 4.2 and Theorem 4.3] for the details.

4.2. Application of the MH solver to the original time-periodic system

Clearly, one could exploit the proposed methodology to solve a time-periodic problem, without applying a parallel-in-time method. More specifically, the (fine) discretization of the periodic system

(27) on $0 = t_0 < t_1 < \dots < t_{N_f} = T$ using implicit Euler's method

$$\left[\frac{1}{\delta T} \mathbf{M} + \mathbf{K}(\mathbf{u}_n) \right] \mathbf{u}_n = \frac{1}{\delta T} \mathbf{M} \mathbf{u}_{n-1} + \mathbf{j}(t_n), \quad n = 1, \dots, N_f \quad (59)$$

with time step size $\delta T = T/N_f$ leads to the system of nonlinear algebraic equations

$$\begin{bmatrix} \mathbf{C} + \mathbf{K}(\mathbf{u}_1) & & & -\mathbf{C} \\ -\mathbf{C} & \mathbf{C} + \mathbf{K}(\mathbf{u}_2) & & \\ & & \ddots & \ddots \\ & & & -\mathbf{C} & \mathbf{C} + \mathbf{K}(\mathbf{u}_{N_f}) \end{bmatrix} \begin{bmatrix} \mathbf{u}_1 \\ \mathbf{u}_2 \\ \vdots \\ \mathbf{u}_{N_f} \end{bmatrix} = \begin{bmatrix} \mathbf{j}(t_1) \\ \mathbf{j}(t_2) \\ \vdots \\ \mathbf{j}(t_{N_f}) \end{bmatrix}, \quad (60)$$

where $\mathbf{C} := \frac{1}{\delta T} \mathbf{M}$. Solution of system (60) arises in the TP-FEM framework, when using the terminology of [1]. We note that the (fine) Euler time step in (60) is much smaller than the (coarse) one in the PP-PC system (28), i.e., $\delta T \ll \Delta T$, which means that system (60) has a much bigger size than (28).

Choosing vector $\mathbf{z} \in \mathbb{R}^d$ in the initial approximation

$$\mathbf{u}^0 := [\mathbf{z}^\top, \mathbf{z}^\top, \dots, \mathbf{z}^\top]^\top \in \mathbb{R}^{N_f d} \quad (61)$$

we obtain the simplified Newton iteration of form (35) for (60)

$$\underbrace{\begin{bmatrix} \mathbf{C} + \mathbf{K}_d(\mathbf{z}) & & & -\mathbf{C} \\ -\mathbf{C} & \mathbf{C} + \mathbf{K}_d(\mathbf{z}) & & \\ & & \ddots & \ddots \\ & & & -\mathbf{C} & \mathbf{C} + \mathbf{K}_d(\mathbf{z}) \end{bmatrix}}_{=: \mathbf{G}_d} \begin{bmatrix} \mathbf{u}_1^{s+1} \\ \mathbf{u}_2^{s+1} \\ \vdots \\ \mathbf{u}_{N_f}^{s+1} \end{bmatrix} = \underbrace{\begin{bmatrix} [\mathbf{K}_d(\mathbf{z}) - \mathbf{K}(\mathbf{u}_1^s)] \mathbf{u}_1^s + \mathbf{j}_1 \\ [\mathbf{K}_d(\mathbf{z}) - \mathbf{K}(\mathbf{u}_2^s)] \mathbf{u}_2^s + \mathbf{j}_2 \\ \vdots \\ [\mathbf{K}_d(\mathbf{z}) - \mathbf{K}(\mathbf{u}_{N_f}^s)] \mathbf{u}_{N_f}^s + \mathbf{j}_{N_f} \end{bmatrix}}_{=: \mathbf{h}^s}. \quad (62)$$

One could then apply MH solver (37) at Newton iteration $s+1$ and solve a linear algebraic system for each harmonic coefficient $\hat{\mathbf{u}}_j^{s+1}$, $j = 1, \dots, N_f$ separately. This is to our best knowledge essentially the same idea as the fixed point method proposed in [9].

When many central processing units (CPUs) are available one may expect the parallelization of the MH frequency domain solution at each Newton iteration (62) to outperform the speed up provided by the parallel-in-time solution on the fine grid in PP-PC (28). Besides, in the linear case TP-FEM solution with the MH transformation effectively solves only one d -dimensional linear system in total, provided sufficient parallelization is possible, i.e., when (at least) N_f processors are

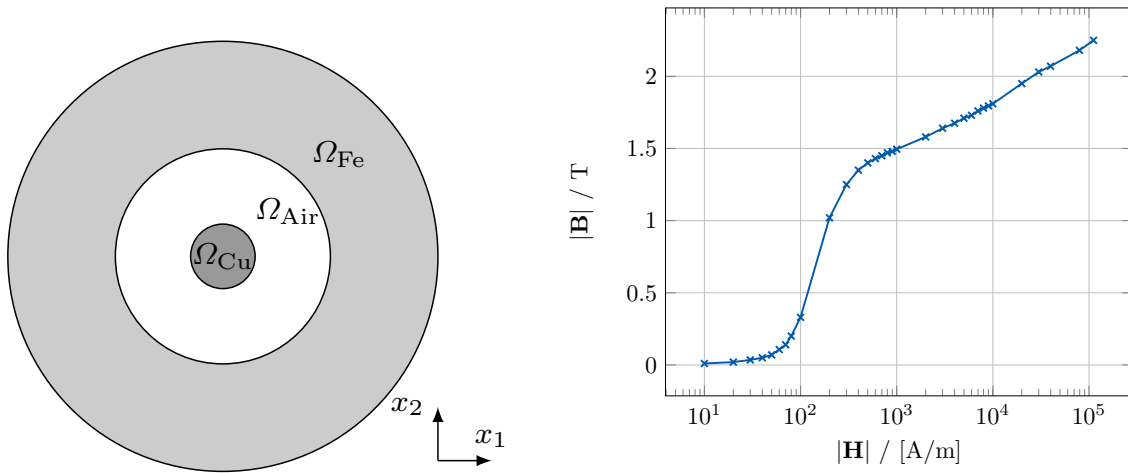


Figure 1: Left: cross-section of a coaxial cable¹. Computational domain consists of tube Ω_{Fe} , conducting wire Ω_{Cu} , and air gap Ω_{Air} in-between. Right: magnetization curve of the ferromagnetic material in Ω_{Fe} given by measured data points.

available. However, we note that application of the MH solver to the PP-PC system and not to (60) is especially beneficial when the number of CPUs is limited ($< N_f$), that is, when one could not calculate each harmonic coefficient $\hat{\mathbf{u}}_j^{s+1}$, $j = 1, \dots, N_f$ in parallel.

5. Numerical experiments

In this section we present the results obtained from application of the proposed (parallel-in-time) algorithm with MH coarse correction to solve the time-periodic problem for a coaxial cable model. Fig. 1 (left) illustrates a sketch of a two-dimensional (2D) domain

$$\bar{\Omega} = \bar{\Omega}_{\text{Fe}} \cup \bar{\Omega}_{\text{Cu}} \cup \bar{\Omega}_{\text{Air}}. \quad (63)$$

It represents the cross-section of the cable, which consists of steel tube Ω_{Fe} , conducting wire Ω_{Cu} , and air gap Ω_{Air} .

The electromagnetic phenomena in the coaxial cable when the inner wire is supplied by a sinusoidal current source are mathematically described by the eddy current problem [22]. In the

¹<http://www.femm.info/wiki/tubeexample>

following subsection we discuss the mathematical modeling of the underlying physical characteristics and describe the properties of the nonlinearity.

5.1. Eddy current problem

A time-periodic eddy current formulation in terms of the magnetic vector potential \vec{A} [22] searches for unknown $\vec{A}(\vec{x}, t)$, with $(\vec{x}, t) \in \Omega \times [0, T]$, which solves

$$\sigma(\vec{x}) \partial_t \vec{A}(\vec{x}, t) + \nabla \times \left(\nu(\vec{x}, |\nabla \times \vec{A}|) \nabla \times \vec{A}(\vec{x}, t) \right) = \vec{j}(\vec{x}, t) \quad \text{in } \Omega \times (0, T), \quad (64)$$

$$\vec{A}(\vec{x}, 0) = \vec{A}(\vec{x}, T), \quad \vec{x} \in \Omega, \quad (65)$$

$$\vec{n} \times \vec{A} = 0 \quad \text{on } \partial\Omega \times [0, T], \quad (66)$$

where $\partial\Omega$ denotes the boundary of Ω and \vec{n} is the outward normal vector to $\partial\Omega$. Function $\sigma(\vec{x}) \geq 0$, $\vec{x} \in \Omega$ describes electric conductivity of the materials. It is positive only for $\vec{x} \in \Omega_{\text{Fe}}$ and is equal to zero in $\Omega \setminus \Omega_{\text{Fe}}$. This gives the parabolic-elliptic character to (64). The sinusoidal current excitation, supplied through the conducting wire defines the RHS

$$\vec{j}(\vec{x}, t) = \mathbb{1}_{\Omega_{\text{Cu}}}(\vec{x}) 100 \sin(2\pi t/T), \quad (\vec{x}, t) \in \Omega \times (0, T), \quad (67)$$

where $\mathbb{1}_{\Omega_{\text{Cu}}}$ denotes the indicator function of subdomain Ω_{Cu} . Determination of the input \vec{j} is more complicated in a three-dimensional case and could be described using winding functions [23]. The magnetic reluctivity $\nu(\vec{x}, |\nabla \times \vec{A}|) > 0$ is defined by the ferromagnetic material in Ω_{Fe} and equals the reluctivity of vacuum $\nu_0 = 10^7/(4\pi)$ H/m in $\Omega \setminus \Omega_{\text{Fe}}$.

The reluctivity function in Ω_{Fe} is determined by the magnetization curve $b : \mathbb{R}_0^+ \rightarrow \mathbb{R}_0^+$, shown in the Fig. 1 (right). It is commonly obtained from measured tuples $(|\vec{B}|, |\vec{H}|)$ so that $|\vec{B}| = b(|\vec{H}|)$, where $|\vec{B}|$ denotes the magnitude of the magnetic flux density \vec{B} and $|\vec{H}|$ is the magnitude of the magnetic field intensity \vec{H} . To obtain a continuously differentiable curve interpolation of the measurement data is performed, e.g., using classical splines or specific approximation techniques as in [24] such that monotonicity is preserved. We can then define the reluctivity

$$\nu(\vec{x}, |\vec{B}|) = \begin{cases} \nu_0, & \vec{x} \in \Omega \setminus \Omega_{\text{Fe}}, \\ \nu(|\vec{B}|), & \vec{x} \in \Omega_{\text{Fe}}. \end{cases} \quad (68)$$

For each $\vec{x} \in \Omega_{\text{Fe}}$ we can construct a continuously differentiable reluctivity function $\nu : \mathbb{R}_0^+ \rightarrow \mathbb{R}_0^+$

from the magnetization curve as [25]

$$\nu(s) = \begin{cases} \frac{b^{-1}(s)}{s}, & s \in \mathbb{R}^+, \\ (b^{-1})'(0), & s = 0. \end{cases} \quad (69)$$

Based on the physical nature of magnetization curve b we can naturally impose the following assumptions on reluctivity ν [25].

Assumption 1 (Conditions on the magnetic reluctivity). *Let for $\nu : \mathbb{R}_0^+ \rightarrow \mathbb{R}_0^+$ it holds:*

- $\nu(t) \geq c_1, t \in \mathbb{R}_0^+$,
- *function $t \mapsto \nu(t)t$ is strongly monotone with monotonicity constant c_1 , see (55),*
- $\nu \in C^1(\mathbb{R}_0^+)$ and $\lim_{t \rightarrow \infty} \nu'(t) = 0$, *which implies that ν is Lipschitz continuous with Lipschitz constant $\kappa_2 := \sup_{t \in \mathbb{R}_0^+} |\nu'(t)|$, as in (56),*
- *function $t \mapsto \nu'(t)t$ satisfies Lipschitz condition (57).*

We will refer to these properties of the nonlinear reluctivity function when applying the simplified Newton algorithm (35) to solve the time-periodic system for (64)-(66).

For numerical solution of (64)-(66) the spatial discretization is performed, e.g., using FEM with linear shape functions [12]. This leads to a time-dependent system of differential-algebraic equations (DAEs) [26], which together with the periodicity constraint has a form of (27), with (singular) mass matrix $\mathbf{M} \in \mathbb{R}^{d \times d}$, nonlinear stiffness matrix $\mathbf{K}(\cdot) : \mathbb{R}^d \rightarrow \mathbb{R}^{d \times d}$ and unknown $\mathbf{u} : [0, T] \rightarrow \mathbb{R}^d$.

We consider $T = 0.02$ s to be the period in the eddy current formulation (64)-(66). In our numerical simulations a spatial discretization of domain Ω with $d = 2269$ degrees of freedom is exploited. The time integration is performed with the implicit Euler method. The DAE is of index-1, therefore in this case it does not need extra care, e.g., with respect to consistent initial values [6]. The time step size $\delta T = 10^{-5}$ s is used for the sequential calculation, for TP-FEM discretization (60), and also as a step size on the fine level of the considered parallel-in-time methods. The coarse propagator solves only one time step per window $[T_{n-1}, T_n]$, $n = 1, \dots, N$, thereby using step size $\Delta T = T/N$. The error used in the termination criterion was calculated for two d -dimensional vectors \mathbf{u} and \mathbf{v} as

$$\varepsilon(\mathbf{u}, \mathbf{v}) = \frac{\|\mathbf{u} - \mathbf{v}\|_2}{\text{aTol} + \text{rTol}\|\mathbf{u}\|_2}, \quad (70)$$

where $\text{aTol} = 10^{-6}$ and $\text{rTol} = 10^{-3}$ were chosen as the absolute and the relative tolerances, respectively. Here $\|\mathbf{u}\|_2$ denotes the Euclidean norm of a vector \mathbf{u} . Calculation is then terminated when the value of ε becomes smaller than 1.

In the following two subsections we illustrate the performance of the MH approach for linear and nonlinear models of the coaxial cable and compare it with existing standard and parallel-in-time approaches.

5.2. Linear model

Let us assume that the reluctivity function ν in (64) is linear, i.e., it does not depend on the solution \vec{A} . We therefore deal with problem (18), where the matrix \mathbf{K} is constant. One could then construct a linear (PP-PC) system of form (20) and directly transform it into the frequency domain (22) [8], thereby solving N separate d -dimensional systems in parallel.

Fig. 2 compares computational costs of several solution approaches in terms of the (effective) number of required linear system solutions. We neglect communication costs in all cases. The figure also shows how the costs of the parallel algorithms scale when the number of processors N increases, while the precision of the fine solution remains unchanged (strong scaling). In particular, the classical time stepping approach, when the solution of the initial value problem is performed sequentially starting from zero initial condition, required time integration over 42 periods until the periodic steady-state solution was reached up to the tolerance specified in (70).

The application of PP-IC (3)-(4) accelerated the sequential calculation up to factor 27 (when using $N = 50$ processors) and with $N = 5$ CPUs the periodic solution was obtained with PP-IC about 6 times faster than with the classical time stepping. The PP-PC method (9) in its turn calculates the periodic solution 29 times quicker compared to the sequential computation already when exploiting only $N = 5$ processing units. However, the disadvantage of this approach is that the computational costs stagnate and there is no further acceleration when applying additional computational power.

In contrast to this, the MH approach applied to PP-PC system (20) as in [8] with $N = 50$ gives the speedup of factor 1 000 and with $N = 5$ of factor 52. Finally, the direct MH solution of the TP-FEM system (60) is performed on the fine grid (with step size $\delta T = 10^{-5}$ s on $[0, 0.02]$ s). It required $N_f = 2000$ separate linear system solves. Clearly, in the linear case the speedup obtained by this approach scales exactly linearly as N grows. In particular, when distributing the workload

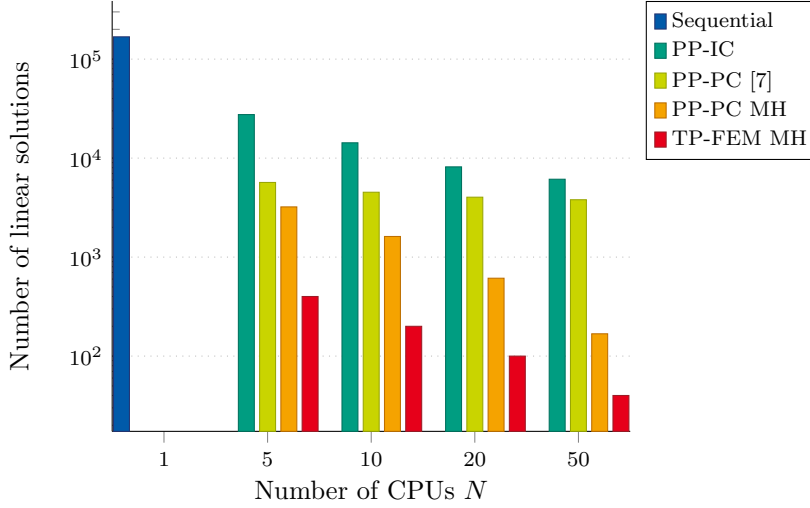


Figure 2: Comparison of the computational costs for different approaches, applied to the linear coaxial cable model: strong scaling.

among $N = 5$ CPUs the acceleration factor is 420 and for $N = 50$ it becomes 4200. Therefore, as expected the TP-FEM solution with the MH approach [9] yields optimal scaling for the solution of the linear time-periodic eddy current problem.

5.3. Nonlinear model

We now present the performance of the iterative method introduced in Section 4 for parallel-in-time solution of a nonlinear time-periodic problem (64)-(66). In this case the nonlinear time-periodic system (28) is solved with the simplified Newton method (31), accompanied by the frequency domain solution at each Newton iteration. The initial guess in (34) for the Newton iteration uses $\mathbf{Z} = \mathbf{0}$, i.e.,

$$\mathbf{U}^0 := \left[(\mathbf{b}_N^{(k)})^\top, (\mathbf{b}_1^{(k)})^\top \dots, (\mathbf{b}_{N-1}^{(k)})^\top \right]^\top$$

is chosen at PP-PC iteration $k + 1$. Analogously to the assumptions of Lemmas 4.5 and 4.6 local convergence of the simplified Newton iteration follows from the conditions of Assumption 1 on reluctivity function ν from (69). Estimate (41) can then be derived based on the results presented in [21].

As in Section 5.2, Fig. 3 illustrates the computational efforts of all the previously described methods to obtain the periodic (steady-state) solution for the nonlinear coaxial cable model. Se-

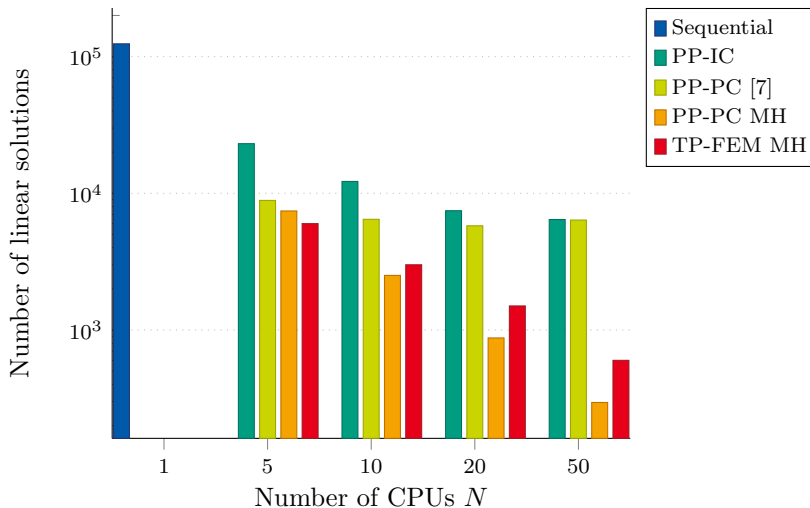


Figure 3: Comparison of the computational costs for different approaches, applied to the nonlinear coaxial cable model: strong scaling.

quential time stepping starting from zero initial value reached the steady-state solution, periodic up to the tolerance given in (70), after calculation over 32 periods. PP-IC computed the periodic solution 19 times faster when using $N = 50$ processors and 5 times faster when $N = 5$. Acceleration using PP-PC iteration (9) amounts to factor 14 with $N = 5$ CPUs and to 19 with $N = 50$ as with PP-IC. As previously seen, the costs of the PP-PC solution do not significantly decrease with the growth of N and even become slightly higher, when comparing the results for $N = 20$ and $N = 50$.

On the other hand, the simplified Newton iteration (31) for PP-PC (28) with MH correction on the coarse grid gives speedup of factor about 16 for $N = 5$ and of factor 420 for $N = 50$. Finally, contrary to the linear case, the TP-FEM MH solution (with $\mathbf{u}^0 = \mathbf{0}$ in (61)) performs worse than PP-PC MH for almost all the considered values of N . More specifically, for 10, 20, and 50 processors the computational costs of TP-FEM MH are higher than those of PP-PC MH, e.g., acceleration factor is equal to 206 when using $N = 50$. A speedup of 20 times is obtained with TP-FEM MH in case of $N = 5$, which is better than that of PP-PC MH (where factor 16 is observed).

6. Conclusions

This paper presents an iterative parallel-in-time solution approach for (nonlinear) time-periodic problems combined with the MH coarse grid correction. The transformation into the frequency do-

main introduces an additional parallelizability on the coarse grid, since the frequency components become decoupled. The proposed simplified Newton method with a special choice of the initial approximation keeps the nonlinearity constant over the Newton iterations and among the time instants, thereby letting the MH frequency domain approach be applicable at each iteration. Convergence of the iterative algorithm has been analyzed and derived from the assumptions imposed on the nonlinearity. Performance of the method is illustrated for the time-periodic eddy current problem for both linear and nonlinear models of a coaxial cable. Superiority of the MH solver over several existing (parallel-in-time) time-domain approaches is shown based on the computational costs calculated in terms of the number of required effective linear system solutions.

Acknowledgements

The authors would like to thank Herbert De Gersem for the multiple fruitful discussions on the multi-harmonic solution approach.

Funding: This research was supported by the Excellence Initiative of the German Federal and State Governments and the Graduate School of Computational Engineering at Technische Universität Darmstadt, as well as by DFG grant SCHO1562/1-2 and BMBF grant 05M2018RDA (PASIROM).

References

References

- [1] T. Hara, T. Naito, J. Umoto, Time-periodic finite element method for nonlinear diffusion equation, *IEEE Trans. Magn.* 21 (5) (1985) 2261–2264.
- [2] J. Stoer, R. Bulirsch, *Numerische Mathematik 2*, 3rd Edition, Springer, Berlin, 2005.
- [3] J.-L. Lions, Y. Maday, G. Turinici, A parareal in time discretization of PDEs, *Comptes Rendus de l'Académie des Sciences – Series I – Mathematics* 332 (7) (2001) 661–668. doi:10.1016/S0764-4442(00)01793-6.
- [4] M. J. Gander, S. Vandewalle, On the superlinear and linear convergence of the parareal algorithm, in: *Domain decomposition methods in science and engineering XVI*, Vol. 55 of *Lecture Notes in Computational Science and Engineering*, Springer, Berlin, 2007, pp. 291–298.

- [5] M. J. Gander, E. Hairer, *Nonlinear Convergence Analysis for the Parareal Algorithm*, Springer Berlin Heidelberg, Berlin, Heidelberg, 2008, pp. 45–56. doi:10.1007/978-3-540-75199-1_4.
- [6] S. Schöps, I. Niyonzima, M. Clemens, Parallel-in-time simulation of eddy current problems using parareal, *IEEE Trans. Magn.* 54 (3) (2018) 1–4. arXiv:1706.05750, doi:10.1109/TMAG.2017.2763090.
- [7] M. J. Gander, Y.-L. Jiang, B. Song, H. Zhang, Analysis of two parareal algorithms for time-periodic problems, *SIAM J. Sci. Comput.* 35 (5) (2013) A2393–A2415. doi:10.1137/130909172.
- [8] I. Kulchytska-Ruchka, H. De Gerssem, S. Schöps, An efficient steady-state analysis of the eddy current problem using a parallel-in-time algorithm, in: *The Tenth International Conference on Computational Electromagnetics (CEM 2019)*, Edinburgh, UK, 2019. arXiv:1905.13076. URL <https://events.theiet.org/cem/>
- [9] O. Bíró, K. Preis, An efficient time domain method for nonlinear periodic eddy current problems, *IEEE Trans. Magn.* 42 (4) (2006) 695–698.
- [10] F. Bachinger, U. Langer, J. Schöberl, Numerical analysis of nonlinear multiharmonic eddy current problems, *Numer. Math.* 100 (4) (2005) 593–616. doi:10.1007/s00211-005-0597-2.
- [11] L. N. Trefethen, *Finite Difference and Spectral Methods for Ordinary and Partial Differential Equations*, Cornell University, 1996.
- [12] S. C. Brenner, L. R. Scott, *The mathematical theory of finite element methods*, 3rd Edition, Vol. 15 of *Texts in applied mathematics*, Springer, New York, 2008.
- [13] D. Bast, I. Kulchytska-Ruchka, S. Schöps, O. Rain, Accelerated steady-state torque computation for induction machines using parallel-in-time algorithms (2019). arXiv:1902.08277.
- [14] M. Nakhla, J. Vlach, A piecewise harmonic balance technique for determination of periodic response of nonlinear systems, *IEEE Trans. Circ. Syst.* 23 (2) (1976) 85–91. doi:10.1109/TCS.1976.1084181.
- [15] J. Gyselinck, P. Dular, C. Geuzaine, W. Legros, Harmonic-balance finite-element modeling of electromagnetic devices: a novel approach, *IEEE Trans. Magn.* 38 (2) (2002) 521–524. doi:10.1109/20.996137.

- [16] S. Außerhofer, O. Bíró, K. Preis, An efficient harmonic balance method for nonlinear eddy-current problems, *IEEE Trans. Magn.* 43 (4) (2007) 1229–1232. doi:10.1109/TMAG.2006.890961.
- [17] P. Deuffhard, *Newton methods for nonlinear problems: affine invariance and adaptive algorithms*, Springer, Berlin, 2004.
- [18] M. J. Gander, I. Kulchytska-Ruchka, I. Niyonzima, S. Schöps, A new parareal algorithm for problems with discontinuous sources, *SIAM J. Sci. Comput.* 41 (2) (2019) B375–B395. arXiv:1803.05503, doi:10.1137/18M1175653.
- [19] E. Zeidler, *Nonlinear Functional Analysis and its Applications II/A. Linear Monotone Operators*, Springer-Verlag, New York Inc., 1990.
- [20] J. M. Ortega, W. C. Rheinboldt, *Iterative Solution of Nonlinear Equations in Several Variables*, 2nd Edition, Society for Industrial and Applied Mathematics, Philadelphia, PA, USA, 2000. doi:10.1137/1.9780898719468.
- [21] C. Pechstein, *Multigrid-Newton-methods for nonlinear-magnetostatic problems*, Master’s thesis, Universität Linz, Linz, Austria (2004).
- [22] J. D. Jackson, *Classical Electrodynamics*, 3rd Edition, Wiley & Sons, New York, 1998. doi:10.1017/CB09780511760396.
- [23] S. Schöps, H. De Gersem, T. Weiland, Winding functions in transient magnetoquasistatic field-circuit coupled simulations, *COMPEL* 32 (6) (2013) 2063–2083. doi:10.1108/COMPEL-01-2013-0004.
- [24] C. Pechstein, B. Jüttler, Monotonicity-preserving interproximation of b-h-curves, *J. Comput. Appl. Math.* 196 (1) (2006) 45–57. doi:10.1016/j.cam.2005.08.021.
- [25] B. Heise, Analysis of a fully discrete finite element method for a nonlinear magnetic field problem, *SIAM J. Numer. Anal.* 31 (3) (1994) 745–759.
URL <http://www.jstor.org/stable/2158028>
- [26] R. Lamour, R. März, C. Tischendorf, *Differential-Algebraic Equations: A Projector Based Analysis*, *Differential-Algebraic Equations Forum*, Springer, Heidelberg, 2013. doi:10.1007/978-3-642-27555-5.